JOURNAL OF GEOPHYSICAL RESEARCH, VOL. 115, C12020, doi:10.1029/2010JC006225, 2010

Volume, heat, and freshwater transports from the South China Sea to Indonesian seas in the boreal winter of 2007–2008

Guohong Fang,[1] R. Dwi Susanto,[2] Sugiarta Wirasantosa,[3] Fangli Qiao,[1] Agus Supangat,[3] Bin Fan,[1] Zexun Wei,[1] Budi Sulistiyo,[3] and Shujiang Li[1]

Received 23 February 2010; revised 18 August 2010; accepted 31 August 2010; published 7 December 2010.

[1] Acoustic Doppler current profiler observations were carried out at two stations along a transect northwest of the Karimata Strait from December 2007 to November 2008. One month and 10 months of full-depth current data were obtained at the western and eastern stations, respectively. The observations show that the South China Sea (SCS) water flows persistently to the Indonesian seas (ISs) in boreal winter. On the basis of current, temperature, and salinity observations by conductivity-temperature-depth casts and bottom-mounted sensors, the volume, heat, and freshwater transport from the SCS to ISs in the month from 13 January to 12 February 2008 are estimated to be 3.6 ± 0.8 Sv (Sv = 10^6 m^3/s), 0.36 ± 0.08 PW, and 0.14 ± 0.04 Sv, respectively. The corresponding transport-weighted temperature is 27.99°C. A downward sea surface slope from north to south at the study area in boreal winter is also found. The observations confirm the existence of the SCS branch of the Pacific-to-Indian-Ocean throughflow in boreal winter and the reversal of the Karimata Strait transport in boreal summer. The seasonal variability in the Karimata Strait transport can exceed 5 Sv. It is proposed that the Karimata Strait throughflow plays a double role in the total Indonesian Throughflow transport, which is especially evident in boreal winter. The negative effect of the double role is reducing the Makassar Strait volume and heat transports; the positive effect is that the Karimata Strait throughflow itself can contribute volume and heat transports to the total Indonesian Throughflow.

Citation: Fang, G., R. D. Susanto, S. Wirasantosa, F. Qiao, A. Supangat, B. Fan, Z. Wei, B. Sulistiyo, and S. Li (2010), Volume, heat, and freshwater transports from the South China Sea to Indonesian seas in the boreal winter of 2007–2008, *J. Geophys. Res.*, *115*, C12020, doi:10.1029/2010JC006225.

1. Introduction

[2] The South China Sea (SCS) is one of largest marginal seas in the world, and the Indonesian seas (ISs) are a major passage linking the Pacific and Indian oceans. The SCS and ISs are connected through the Karimata and Gaspar Straits. A number of numerical studies [*Metzger and Hurlbut*, 1996; *Lebedev and Yaremchuk*, 2000; *Fang et al.*, 2002, 2005, 2009; *Tozuka et al.*, 2007, 2009;*Yaremchuk et al.*, 2009] have revealed that the circulations in SCS and ISs are closely linked mainly through the Karimata Strait (for short the Gaspar Strait is included in the Karimata Strait in this paper for its narrowness). *Fang et al.* [2002, 2005, 2009] proposed that the SCS is an important passage for the Pacific water to flow into the Indian Ocean and a SCS branch of the Pacific-to-Indian-Ocean throughflow exists in boreal wintertime. *Gordon et al.* [2003] proposed that the less saline water from the Java Sea, which can be traced back to the SCS through the Karimata Strait, blocked the upper layer outflow from the Makassar Strait in boreal winter, resulting in a cool Indonesian Throughflow (ITF). They found that the observed transport-weighted temperature of the Makassar Strait throughflow was 15°C, rather than the previously estimated 24°C. *Qu et al.* [2005, 2009] and *Tozuka et al.* [2007, 2009] proposed that a SCS throughflow exists in the SCS and has great impact on the ITF. Moreover, *Tozuka et al.* [2009] found that the volume and heat transport of the Makassar Strait throughflow in numerical experiment are reduced by 1.7 Sv and 0.19 PW, respectively, by the existence of the SCS throughflow. Many other studies [e.g., *Wang et al.*, 2006; *Yu et al.*, 2007] have also investigated the SCS throughflow recently. However, the validity of conclusions of all the above studies strongly relies on a sufficient magnitude of the transport though the Karimata Strait.

[3] So far the only observation-based estimation of Karimata Strait transport was done nearly 50 years ago by *Wyrtki* [1961], who estimated the winter transport in the Karimata Strait is up to 4.5 Sv, from the SCS to the Java Sea; and the summer transport is up to 3 Sv, but from the Java Sea to the SCS. Using sea surface height and ocean

[1]Key Laboratory of Marine Science and Numerical Modeling, The First Institute of Oceanography, State Oceanic Administration, Qingdao, China.
[2]Lamont-Doherty Earth Observatory, Earth Institute at Columbia University, Palisades, New York, USA.
[3]Agency for Marine and Fisheries Research, Ministry of Marine Affairs and Fisheries, Jakarta, Indonesia.

0148-0227/10/2010JC006225

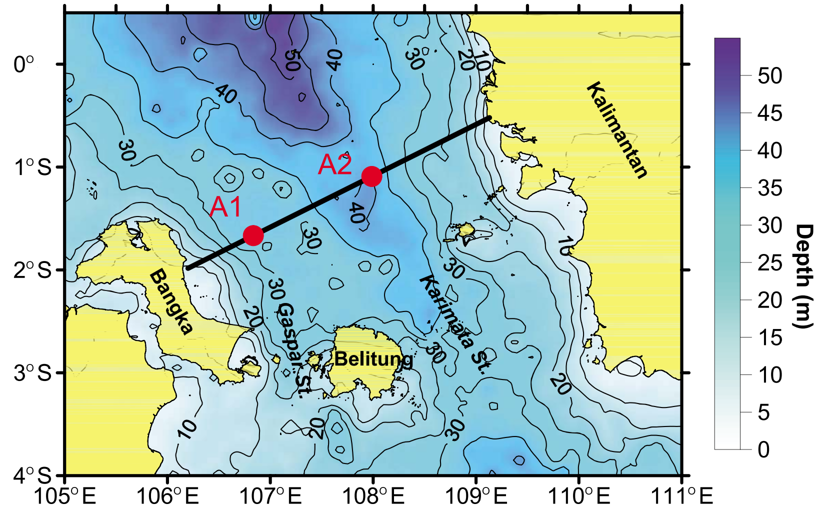

Figure 1. Trawl-resistant bottom mount sites A_1 and A_2 (red dots). Black line is the location of section A. Isobaths (in meters) are digitized to 5′ × 5′ from the nautical chart published by the *Indonesian Hydro-Oceanographic Service* [2006].

bottom pressure measured by satellites, *Song* [2006] estimated the total volume transport through the Karimata and Makassar straits to be 7.5 Sv. Since the ship drift data, as used by *Wyrtki* [1961], usually contain great uncertainty, and the Karimata Strait transport was not separated from the Makassar Strait transport in Song's estimation, reliable observation-based estimates of the transports through the Karimata Strait are so far not available. In addition, numerical model results for Karimata Strait transport still contain great uncertainty. For example, *Lebedev and Yaremchuk* [2000], *Fang et al.* [2005], and *Yaremchuk et al.* [2009] give 4.4, 4.4, and 1.3 Sv, respectively, for boreal winter, and 2.1, 1.3, and 0.3 Sv, respectively, for annual mean. *Tozuka et al.* [2009] and *Fang et al.* [2009] give annual means of 1.6 and 1.2 Sv, respectively. Therefore, to obtain a more reliable value for the Karimata Strait transport, direct current measurement with modern instruments is necessary.

[4] This paper describes observations at two current stations along a transect north of the Karimata Strait carried out from December 2007 to November 2008, which is supported by the program of "The SCS–Indonesian Seas Transport/Exchange (SITE) and Impact on Seasonal Fish Migration," established jointly by the scientists from China, Indonesia, and the United States in October 2006 [see also *Susanto et al.*, 2010]. Since current data at one station are obtained only in the boreal winter of 2007–2008, the present paper mainly focuses on the currents and transports in wintertime. In addition to local wind forcing, along-current sea surface slope is also evaluated to confirm the validity of "island rule" mechanism [*Godfrey*, 1989] on the generation of the SCS branch of the Pacific to Indian Ocean throughflow.

2. Field Measurements

[5] A cross-strait section (hereafter referred to as section A) was selected at about 150 km north of Belitung in the southern Natuna Sea between northeast coast of Banka and west coast of Kalimantan for measuring transport between the SCS and ISs, where the topography is relatively flat. Three trawl-resistant bottom mounts (TRBMs) were deployed along the section, but the current data were successfully obtained only from two sites, which are designated as A_1 (1°40.0′S, 106°50.1′E) and A_2 (1°05.6′S, 107°59.2′E), respectively (Figure 1). The length of section A is about 360 km and the mean depth is around 32 m.

[6] The TRBM at A_1 was equipped with a LinkQuest Inc. 600 kHz acoustic Doppler current profiler (ADCP), an RBR Ltd. temperature-pressure logger, two acoustic releases, an acoustic modem, and a marine location beacon. The TRBM at A_2 carries the exact same equipments as the one at A_1 except an additionally installed Sea-bird conductivity-temperature-pressure (CTP) recorder. The acoustic modem on each TRBM is used to communicate with a ship deck unit to set ADCP measurement parameters or retrieve ADCP data in case TRBM cannot be recovered.

[7] The TRBM at A_2 was deployed on 4 December 2007 and recovered on 1 November 2008. The TRBM at A_1 was deployed on 12 January 2008 and recovered on 9 May 2008. Conductivity-temperature-depth (CTD) casts were taken during the deployment and recovery cruises. Pressure measurements from recovered TRBMs show that the averaged depths at A_1 and A_2 are 36.6 and 48.0 m, respectively.

3. Current Data Analysis and Volume Transport Estimation

3.1. Observed Subtidal Currents at A_1 and A_2

[8] The ADCP data obtained from TRBM at A_2 covers period of 4 December 2007 to 1 November 2008 with about one month gap from 12 January to 15 February 2008 due to the failure in setting ADCP measurement parameters in January 2008 cruise. The ADCP data obtained from A_1 is only about one month long, from 12 January to 13 February 2008. The vertical bin sizes of ADCP measurements are 1 m for A_1 and 2 m for A_2. The sampling time intervals are 20 min for A_1, and 10, 20, and 40 min for A_2 in the periods of 4 December 2007 to 12 January 2008, 15 February to 10 May 2008, and 11 May to 1 November 2008, respectively.

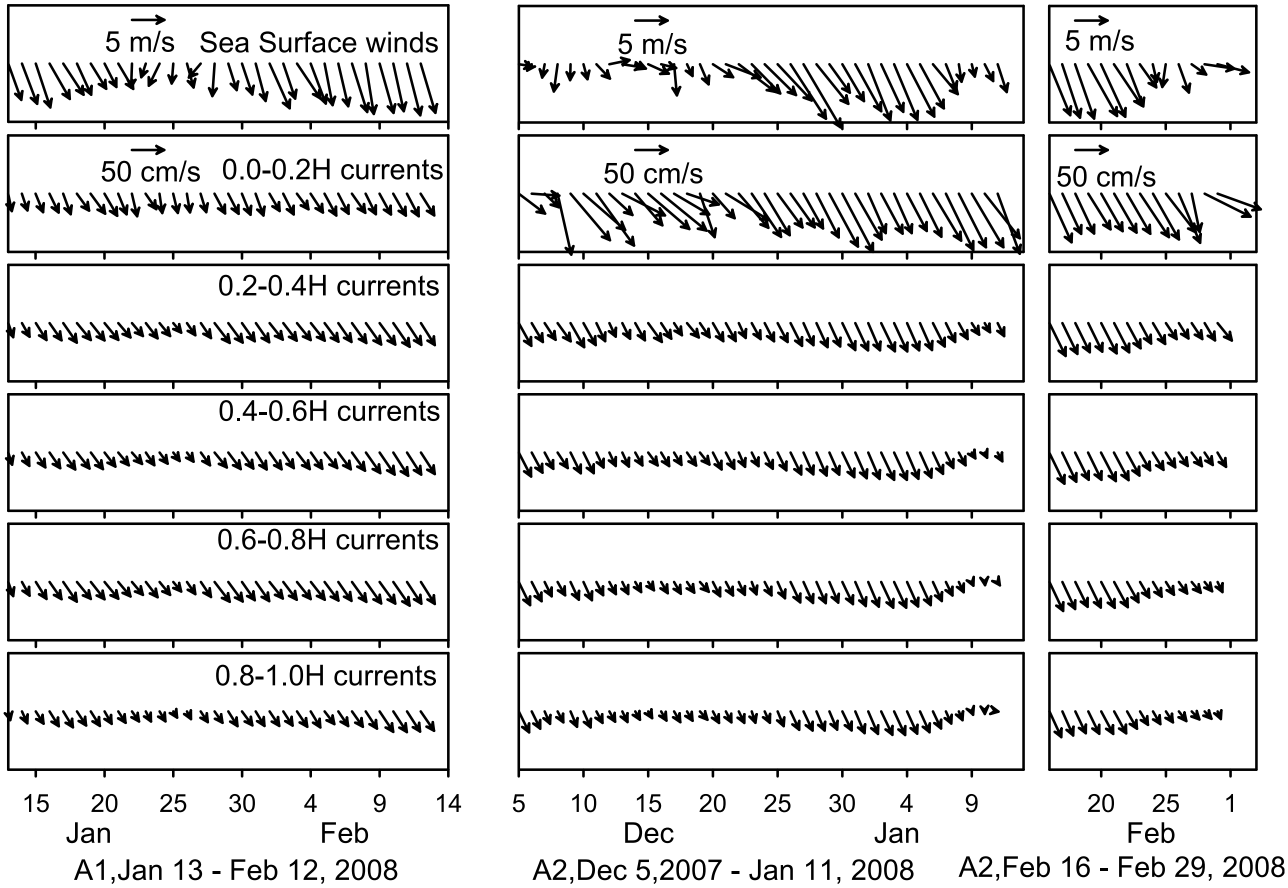

Figure 2. Daily mean surface winds and observed daily mean currents at sites A_1 and A_2 in the boreal winter of 2007–2008. H is the water depth at the ADCP sites: 36.6 m for A_1 and 48.0 m for A_2.

The daily mean (25 h mean) currents at 10 equally spaced layers from sea surface to bottom are calculated from the measurements of ADCP, then the data of the uppermost layer are replaced with the values linearly extrapolated from the second and third layers according to constant shear assumption [e.g., *Sprintall et al.*, 2009], given the problem caused by surface reflection contamination of the ADCP. The winds that are used to establish the relationship with the observed currents are QSCAT (Quick Scatterometer) and NCEP (National Centers for Environmental Prediction) blended 10 m surface winds obtained from the Research Data Archive (data available at http://www.cora.nwra.com/~morzel/blendedwinds.qscat.ncep.html) maintained by the Computational and Information Systems Laboratory at the National Center for Atmospheric Research [*Milliff et al.*, 1999]. The daily mean current vectors of five layers (vertically averaged every two layers) from 13 January to 12 February 2008 at A_1 and those from 5 December 2007 to 11 January 2008 and 16–29 February 2008 at A_2, together with daily mean winds, are plotted (Figure 2).

[9] It can be seen that the currents during this period are persistently toward the southeast from surface to bottom at both A_1 and A_2. The current speeds in upper layers are greater than those in lower layers, and the current gets stronger when northwesterly winds are stronger, suggesting that the winds are the dominant forcing of the currents. However, the southeastward currents still exist while the northwesterly winds diminish, implying the presence of downstream sea surface slope in the study area. The magnitude of this downstream slope will be estimated in section 5.

3.2. Regression of Currents on Winds at A_2

[10] Since there are no simultaneous observed current data at A_1 and A_2, we have to fill up data gap of either A_1 or A_2 to estimate the transports through section A. Because the current data at A_2 are much longer than those at A_1, filling up the data gaps of A_2 is more feasible and reasonable. By visual inspection of the current and wind variabilities shown in Figure 2, one can see that they correlate very well. Therefore, we can take advantage of this correlation to derive the time series of currents at A_2 from the continuous wind data by means of regression analysis.

[11] Since the major concern of the present study is the transport rates of water mass, heat, and freshwater across section A, we decompose the current vectors into an along-channel component, u, which is perpendicular to section A (positive southeastward), and a cross-channel component, v, which is parallel to section A (positive northeastward). The u and v can be calculated from

$$\begin{cases} u = w\cos(\theta - \psi) \\ v = -w\sin(\theta - \psi), \end{cases} \tag{1}$$

Table 1. Regression Parameters of Along-Channel Currents on Local Winds[a]

Layer	u_0 (cm/s)	a (10^{-2})	b (10^{-2})	r
1	1.7	13.27	−1.25	0.83
2	7.2	9.11	−0.77	0.87
3	12.8	4.95	−0.30	0.83
4	13.3	4.41	−0.10	0.79
5	13.0	3.93	0.09	0.77
6	12.4	3.32	0.25	0.75
7	12.4	2.58	0.31	0.70
8	13.0	1.83	0.17	0.63
9	12.0	1.50	−0.07	0.63
10	10.3	1.47	−0.13	0.68

[a]The u_0 is intercept value, representing along-channel velocity when local wind is zero, a and b are regression coefficients, and r is correlation coefficient.

where w and θ are the speed and direction of the current, respectively, and ψ is the normal direction of section A, which is equal to 154° referenced to true north.

[12] We assume that the variability of along-channel current component is mainly caused by the variation of local winds, and can thus be empirically expressed as

$$u = u_0 + a\,U + b\,V + \varepsilon, \tag{2}$$

where U and V are the along-channel and the cross-channel components of sea surface winds at A_2, u_0 is the intercept value, representing along-channel current velocity without local winds, a and b are the regression coefficients, ε is the residual. Full observed daily mean along-channel current velocities of each layer at A_2 and the corresponding sea surface winds are used in the regression analysis. The obtained intercept value, regression coefficients, and correlation coefficient for each layer are shown in Table 1. We can see that u_0 is nearly independent of depth, with an average of 10.8 cm/s. The coefficient a decreases with depth and is much greater than the coefficient b, indicating that the variability of along-channel currents becomes smaller toward the seabed and is basically induced by the variation of along-channel wind component. The correlation coefficient r is generally high, suggesting that the derived regression equation can be used to interpolate or extrapolate along-channel currents when observations are not available. We did exactly same analysis using the current and wind stress, instead of wind velocity itself, and found that the correlation r ranges from 0.70 to 0.78 in the three uppermost layers, smaller than those in Table 1, thus the results are not adopted for current interpolation.

[13] Figure 3 displays the comparison between the time series of observed (blue line) and regression-derived (red line) vertically averaged along-channel current velocities at A_2. It can be seen that they agree well. Monthly mean values calculated from these two time series are given in Table 2. These monthly values are also plotted in Figure 3, in which the red and blue dots denote derived and observed velocities, respectively, with open blue dots indicating that the observed data are not complete in the corresponding months. Differences between the derived monthly means and the observed ones are also given in Table 2. The root-mean-square (RMS) value of the differences is equal to 5.7 cm/s, which is significantly smaller than the monthly velocities themselves.

[14] The monthly mean velocities listed in Table 2 show that the flows are from the SCS to ISs from October to the following March, but in opposite direction from April to September. Since the flows from SCS to ISs are relatively stronger, annual mean flow along the channel is still southward. The vertical profiles of the time-averaged along-channel current velocities observed at A_1 and derived at A_2 over the period from 13 January to 12 February are shown in Figure 4. The vertically averaged velocities of A_1 and A_2 are 29.3 and 35.0 cm/s, respectively. One can see that the velocity profile at A_2 constructed by linear regression is reasonable and can be used in the following transport estimation. From the RMS difference between observation and prediction given in Table 2, which is 5.7 cm/s, the mean value of the derived vertically averaged velocity at A_2 from 13 January to 12 February 2008 may contain a relative RMS error of ~16%.

3.3. Volume Transport

[15] The volume transport through the Karimata Strait, F_V, can be estimated using the following formula:

$$F_V = \int_A u\,dA, \tag{3}$$

where dA denotes the area element of section A. The daily values of u from 13 January to 12 February 2008 on the section are interpolated or extrapolated layer by layer along terrain-following surfaces from the daily values at A_1 and A_2. The bathymetry along the section used here is based on the nautical chart published by the *Indonesian Hydro-Oceanographic Service* [2006], with minor adjustment near A_1 and A_2 based on bottom pressure observations at these

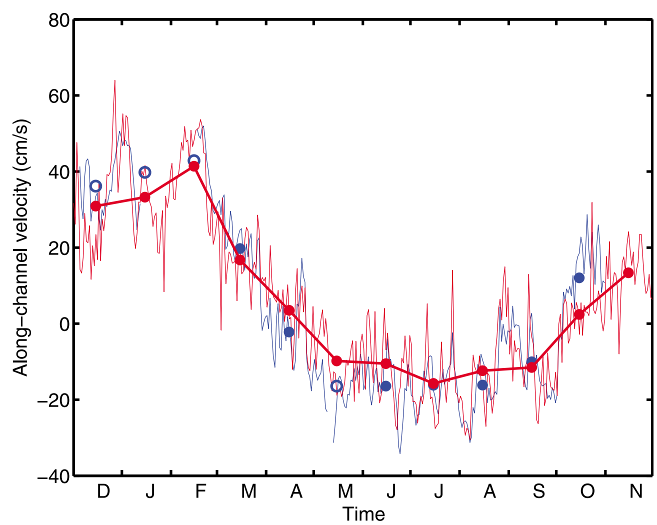

Figure 3. Comparison of the observed and regression-derived vertically averaged along-channel current velocities at A_2. Positive (negative) values are southeastward (northwestward) flows. Blue line indicates the observed values; red line indicates the derived values by linear regression analysis. Blue and red dots are monthly mean velocities. Open blue dots indicate that the observations are not complete in the corresponding months.

Table 2. Comparison of the Regression-Derived Monthly Vertically Averaged Along-Channel Current Velocities (cm/s) at A_2 to the Observed Ones[a]

	Month												
	1	2	3	4	5	6	7	8	9	10	11	12	Mean
Derived from regression	33.2	41.4	16.7	3.5	−9.8	−10.5	−15.7	−12.4	−11.5	2.4	13.4	30.9	6.8
Observed	39.8	42.9	19.7	−2.2	−16.4	−16.4	−16.2	−16.2	−10.0	12.0	(24.1)	36.2	8.1
Difference	−6.6	−1.5	−3.0	5.7	6.6	5.9	0.5	3.8	−1.5	−9.6	(−10.7)	−5.3	−1.3
Days of observation	11	14	31	30	31	30	31	31	30	31	0	27	

[a]RMS of differences is 5.7. The observed mean velocity of November is interpolated from October and December.

two stations. Four interpolation/extrapolation schemes were tested: (1) linear interpolation/extrapolation along the section, (2) evenly dividing the distance between stations A_1 and A_2 with velocities uniformly assigned by those at the nearest stations, (3) cubic-spline interpolation with no slip condition at sidewalls, and (4) logarithmic-profile-cubic-spline interpolation with no slip condition at sidewalls. The first three schemes have been used by *Sprintall et al.* [2009] before, and the fourth scheme is described in detail in Appendix A. Using the interpolated/extrapolated along-channel velocities obtained from each of the four schemes, daily volume transport values were calculated according to equation (3), yielding mean volume transports of 3.8, 3.8, 3.4, and 3.6 Sv for the four schemes, respectively. These results show that the uncertainty of mean volume transport estimate due to the difference of the interpolation/extrapolation method is about 0.2 Sv, or about 6% of the transport. Since the value obtained from the logarithmic-profile-cubic-spline interpolation scheme, 3.6 Sv, is close to the average of the four schemes, the result based on this scheme is adopted in the present study. The daily volume transport has a standard deviation of 0.8 Sv and is shown in Figure 5a. The sectional distribution of mean along-channel velocity in the month from 13 January to 12 February 2008 is shown in Figure 8a.

[16] As stated in section 2.2, the regression-derived velocities at A_2 may contain a RMS error of ~16%. We have tested the influence of the velocity errors of A_2 on the volume transport estimate, and found that these errors can cause errors with standard deviation of ~10% in the estimated volume transport. The combination of errors induced by derivation of velocities at A_2 and interpolation/extrapolation of velocities to section A can cause an uncertainty of ~0.4 Sv in the mean volume transport estimate.

4. Heat and Freshwater Transports

[17] The heat transport through the Karimata Strait, F_H, can be calculated from

$$F_H = \rho C_p \int_A (T - T_0) u dA, \quad (4)$$

where ρ is the water density, taken to be 1021 kg m^{-3} for a mean temperature of 28°C and a mean salinity of 33, C_p is the specific heat, ρC_p can be regarded as the heat capacity per unit volume and is taken to be 4.1×10^6 J m^{-3} K^{-1} for the above temperature and salinity, T is the water temperature, and T_0 is a reference temperature. The choice of reference temperature is somewhat arbitrary [*Schiller et al.*, 1998]. It is more desirable to use the transport-weighted mean temperature of the corresponding return flow as the reference temperature. However, it is hard to determine which flow is the corresponding return flow. In calculation of the heat transport of the ITF, *Schiller et al.* [1998] used 3.72°C as reference temperature, which is the mean temperature of the water across the meridional vertical section from southern Tasmania to 50°S. This value was also adopted by *Ffield et al.* [2000]. To facilitate a comparison of the SCS interocean heat transport to the ITF heat transport, the reference temperature, 3.72°C, is also adopted in this study. Using equations (3) and (4), a transport-weighted temperature can be inversely calculated from

$$T_T = F_H \left(\rho C_p F_V\right)^{-1} + T_0. \quad (5)$$

The salt and freshwater transports through the Karimata Strait, F_S and F_W, can be calculated from

$$F_S = \rho \int_A S u dA, \quad (6)$$

$$F_W = \int_A [(S_0 - S)/S_0] u dA, \quad (7)$$

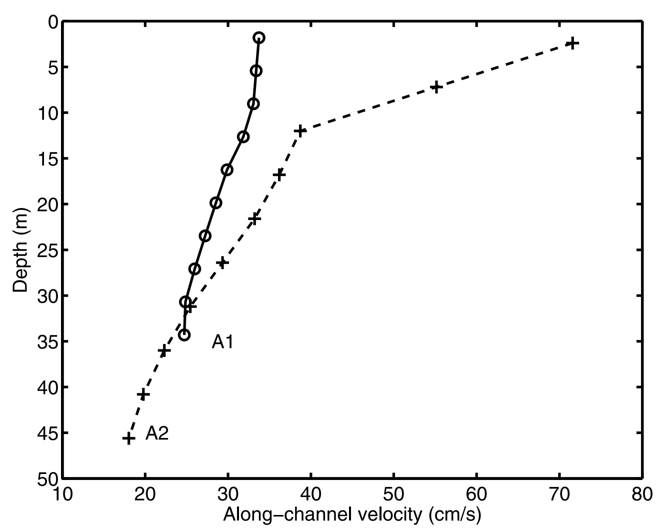

Figure 4. Vertical profiles of time-averaged along-channel currents at A_1 and A_2 in the month from 13 January to 12 February 2008. A_1 and A_2 profiles are based on observation and regression, respectively.

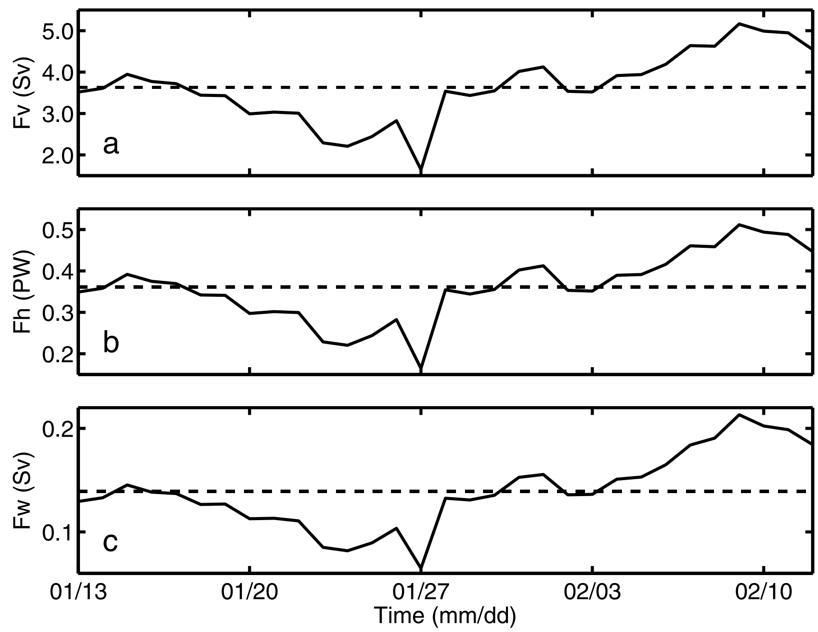

Figure 5. Time series of the (a) volume, (b) heat, and (c) freshwater transports from the SCS to ISs during the month from 13 January to 12 February 2008. The mean volume, heat, and freshwater transports are 3.6 Sv, 0.36 PW, and 0.14 Sv, respectively, as indicated by dashed lines. The corresponding standard deviations are 0.8 Sv, 0.08 PW, and 0.04 Sv, respectively.

respectively, where S is salinity and S_0 is reference salinity. To make our estimation consistent, same meridional section from southern Tasmania to 50°S is selected to obtain the reference salinity, which is 34.62 on the basis of the climatological data set of *Levitus and Boyer* [1994].

[18] The temperature and salinity observations available to us include vertical profiles from CTD casts on 3–4 December 2007 and 14–15 February 2008 at A_1 and A_2, and time series of bottom temperature and salinity from the temperature-pressure logger at A_1 and the CTP recorder at A_2. The CTD temperature and salinity profiles are shown in Figure 6, in which the near-seabed segments indicated by dashed lines are linearly extrapolated from the observations in a 10 m range above these segments. From Figure 6 one can see that the water in this season is generally well mixed (the variations of ~0.2°C in temperature and ~0.1 in salinity near the sea surface on 3–4 December 2007 are caused by heavy rain during the cruise). Temperatures at A_1 are higher than those at A_2, while salinities at A_1 are lower. The observed bottom temperatures during the boreal wintertime at both A_1 and A_2 are displayed in Figure 7a. The observed bottom salinities at A_2 are given in Figure 7b. Bottom salinities at A_1 are inferred through the following procedure: We first calculate the bottom salinity difference between A_1 (from CTD) and A_2 (from CTP recorder) on 3 December 2007 and 14 February 2008. Then the bottom salinity differences at times between the above two dates are linearly interpolated from those two differences on 3 December 2007 and 14 February 2008. Finally, the time series of bottom salinity at A_1 is obtained by adding the interpolated differences to the bottom salinities at A_2., and is shown in Figure 7b.

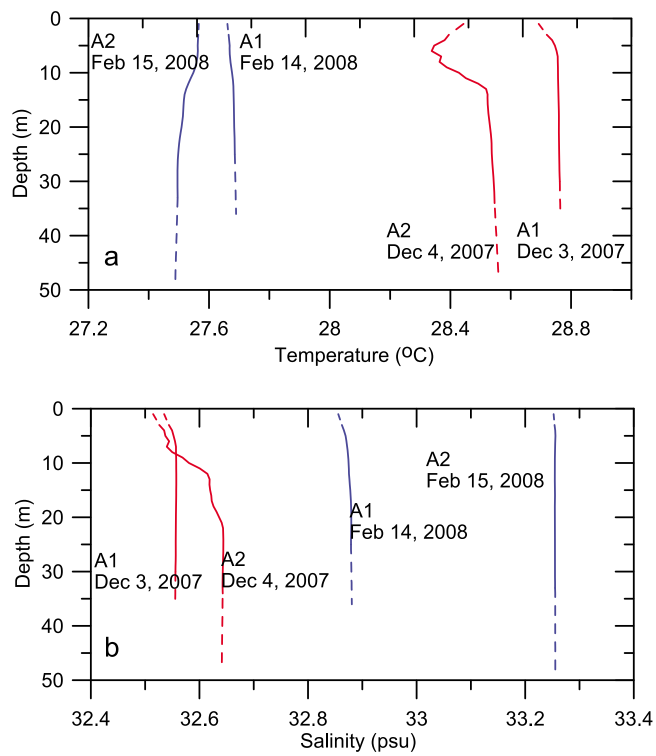

Figure 6. (a) Temperature profiles and (b) salinity profiles from four CTD casts. Red and blue lines indicate the measurements taken on 3–4 December 2007 and 14–15 February 2008, respectively. Solid and dashed segments of the profiles indicate the observed and extrapolated values, respectively.

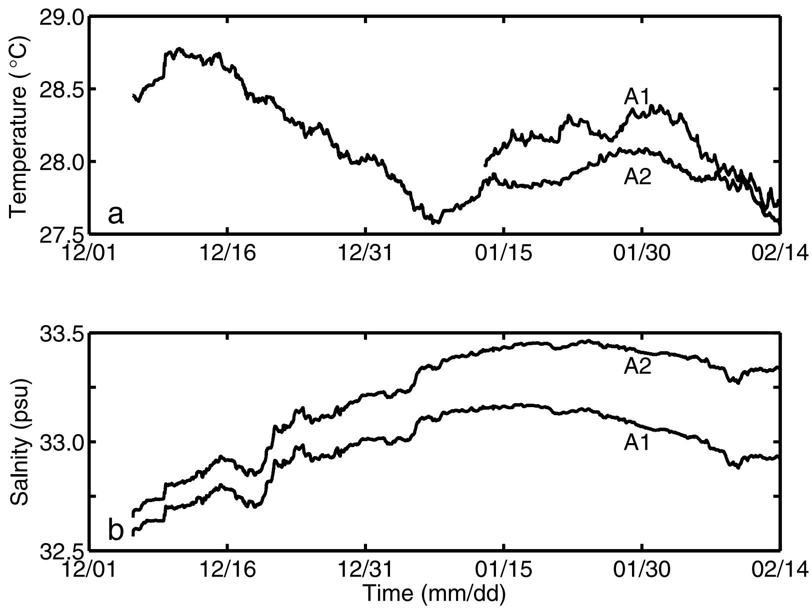

Figure 7. Time series of (a) temperature and (b) salinity at seabed. The temperatures at A_1 and A_2 were measured by RBR temperature and pressure logger and Sea-Bird conductivity-temperature-pressure (CTP) recorder, respectively. The salinities at A_2 were measured with the same CTP recorder, and the salinities at A_1 are inferred from those measured by CTP at A_2 and CTD at A_1.

[19] The temperature at time t and depth z_k, $k = 1, 2, \ldots, 10$, can be linearly interpolated according to the following formula:

$$T(t,z_k) = T(t,z_b) + \frac{t-t_1}{t_2-t_1}[T(t_2,z_k) - T(t_2,z_b)] + \frac{t_2-t}{t_2-t_1}[T(t_1,z_k) - T(t_1,z_b)], \quad (8)$$

where t_1 and t_2 represent the times of CTD casts at A_1/A_2 on 3–4 December 2007 and 14–15 February 2008, respectively, and z_b is the bottom layer depth. With known vertical temperature profiles at A_1 and A_2, the temperatures on section A can then be calculated from an appropriate interpolation/extrapolation scheme. In the present study, three schemes were tested. The first two are the same as those for velocity interpolation/extrapolation; the third scheme is cubic-spline interpolation with zero derivative (no heat transfer) boundary condition at sidewalls. Using the temperatures interpolated/extrapolated from each of the three schemes and the along-channel velocities derived from the logarithmic-profile-cubic-spline interpolation scheme (section 3.3) the heat transport can be calculated from equation (4), and the time-mean values according to the three schemes are 0.361, 0.362, and 0.362 PW, respectively. Since the values are almost the same, we simply adopt the linear scheme as interpolation/extrapolation scheme in the present study. The salt and freshwater transports are calculated similarly. The daily heat and freshwater transport are shown in Figures 5b and 5c, respectively. The sectional distributions of the mean temperature and salinity in the month from 13 January to 12 February are demonstrated in Figures 8b and 8c, respectively. The calculated heat, salt, and freshwater transports as well as transport-weighted temperature for the month from 13 January to 12 February 2008 are listed in Table 3. They are 0.36 ± 0.08 PW, $0.12 \pm 0.03 \times 10^9$ kg s^{-1}, 0.14 ± 0.04 Sv, and 27.99°C, respectively. In Table 3 the volume transport, 3.6 ± 0.8 Sv, obtained in section 3.3 is also given.

5. Along-Channel Sea Surface Slope

[20] *Wyrtki* [1987] found that associated with the ITF, the mean steric height south of Davao is higher than that south of Java by 0.16 m at the sea surface. The distance from Davao to Java along the ITF route passing through the Makassar Strait is about 2000 km. Therefore, the mean sea surface height gradient along ITF is about -8×10^{-8}. It is of interest to examine whether there is also a sea surface slope associated with the Karimata Strait throughflow in boreal wintertime. This sea surface slope can be estimated from the following along-channel momentum equation:

$$\partial\bar{u}/\partial t - f\bar{v} = -g\partial\varsigma/\partial x + (\tau_{sx} - \tau_{bx})/\rho H, \quad (9)$$

where $\bar{u}$ and $\bar{v}$ are vertical mean along- and cross-channel current velocities, respectively; g, f, ρ, and H are the constant of gravitation, Coriolis parameter, water density, and water depth, respectively; ς and $\partial\varsigma/\partial x$ are the sea surface height and the along-channel sea surface slope, respectively; and τ_{sx} and τ_{bx} are the along-channel components of wind stress and seabed frictional stress, respectively.

[21] The τ_{sx} and τ_{bx} are related to the sea surface wind and near bottom current as

$$\tau_{sx} = C_{Ds}\rho_a\tau_{sx}^*, \quad \text{with} \quad \tau_{sx}^* = WU, \quad (10)$$

$$\tau_{bx} = C_{Db}\rho\tau_{bx}^*, \quad \text{with} \quad \tau_{bx}^* = w_1u_1, \quad (11)$$

respectively, in which C_{Ds} and C_{Db} are drag coefficients of the wind stress and bottom frictional stress, assumed constants in this study; ρ_a is the air density, taken to be

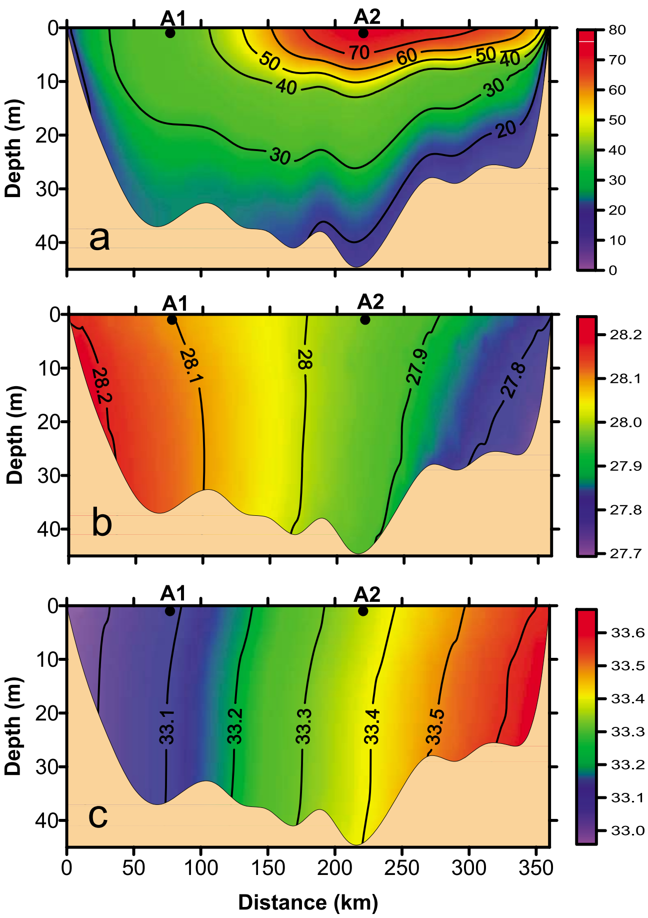

Figure 8. Distributions of mean along-channel (a) velocity, (b) temperature, and (c) salinity on section A for the month from 13 January to 12 February 2008. Bathymetry along the section is based on the nautical chart published by the *Indonesian Hydro-Oceanographic Service* [2006], with minor adjustment near A_1 and A_2 based on bottom pressure observations at these two stations.

1.169 kg m^{-3} for a mean sea level air pressure of 1.01×10^5 Pa and a mean air temperature of 28°C; τ_{sx}^* and τ_{bx}^* are the pseudo stresses; W is the wind speed; and w_1 and u_1 are the current speed and along-channel velocity at 1 m above seabed [e.g., *Csanady*, 1982], respectively. The u_1 can be deduced from velocities of the bottom layer (layer 10 in Table 1) through a logarithmic profile

$$u_1 = u_b \ln(1/z_0)/\ln(z_b/z_0), \qquad (12)$$

where u_b and z_b are the velocity and the mean height above the seabed of the bottom layer, respectively, and z_0 is roughness length parameter.

[22] Equation (9) is applied to the observed daily mean currents from 13 January to 12 February 2008 at A_1, and those from 5 December 2007 to 11 January 2008 and 16–29 February 2008 at A_2. The calculation of RMS of each term in equation (9) indicates that the magnitudes of the terms on the left side of equation are at least 1 order smaller than those on the right side, and can thus be ignored. If only the time-averaged sea surface slope is considered, the momentum equation (9) can be written in the following form

$$\tau_{bx}^* = A + B\tau_{sx}^* + \varepsilon, \qquad (13)$$

where ε is residual, representing the minor terms, and the coefficients A and B are

$$A = (gH/C_{Db})\partial\varsigma/\partial x, \quad B = (\rho_a/\rho)(C_{Ds}/C_{Db}). \qquad (14)$$

Here the sea surface slope is balanced by bottom friction when winds diminish. It follows from the above relations that

$$C_{Db} = \beta C_{Ds}, \quad \partial\varsigma/\partial x = \alpha C_{Ds}, \qquad (15)$$

in which

$$\beta = (\rho_a/\rho)B^{-1}, \quad \alpha = -\beta A/gH. \qquad (16)$$

The regression analysis based on equation (13) yields $A = (145 \pm 68) \times 10^{-4}$ m^2 s^{-2}, $B = (11.3 \pm 1.8) \times 10^{-4}$ for site A_1, and $A = (217 \pm 50) \times 10^{-4}$ m^2 s^{-2}, $B = (8.3 \pm 1.1) \times 10^{-4}$ for site A_2. Inserting these values into equation (16) results in $\beta = 1.02 \pm 0.16$ and $\alpha = -(4.2 \pm 2.6) \times 10^{-5}$ for A_1, and $\beta = 1.38 \pm 0.18$ and $\alpha = -(8.5 \pm 3.0) \times 10^{-5}$ for A_2.

[23] The QSCAT and NCEP blended wind data set uses the following dependence of C_{Ds} on W for calculating wind stresses [*Milliff and Morzel*, 2001]:

$$C_{Ds} = \left(2.70\ W^{-1} + 0.142 + 0.0764\ W\right) \times 10^{-3}, \qquad (17)$$

which gives $C_{Ds} = 1.12 \times 10^{-3}$ for $W = 4$ m/s and $C_{Ds} = 1.18 \times 10^{-3}$ for $W = 10$ m/s. The most (72%) wind speeds in the period from 1 December 2007 to 29 February 2008 are within the range of 4 to 10 m/s, and the rest (27%) are mostly below 4 m/s and the corresponding wind stresses are very small. Therefore, we can use a constant 1.15×10^{-3} for C_{Ds}. This yields $C_{Db} = (1.17 \pm 0.18) \times 10^{-3}$ and $(1.59 \pm 0.23) \times 10^{-3}$ for A_1 and A_2, and $\partial\zeta/\partial x = -(4.8 \pm 3.0) \times 10^{-8}$ and $-(9.8 \pm 3.5) \times 10^{-8}$ for A_1 and A_2, respectively. Although the estimated sea surface slopes at A_1 and A_2 show significant discrepancy, their ranges of variability overlap each other. Thus we can use their mean value, -7×10^{-8}, as a rough estimate for the sea surface slope in the study area, which is equivalent to a sea surface drop of 7 cm in a distance of 1000 km. The magnitude of the sea surface gradient associated with the boreal winter Karimata Strait through-

Table 3. Estimates of Mean Volume, Heat, Salt, and Freshwater Transports With Corresponding Standard Deviations and of Mean Transport-Weighted Temperature for the Month From 13 January to 12 February 2008[a]

	Volume Transport	Heat Transport	Salt Transport	Freshwater Transport	Transport-Weighted Temperature
Estimate	3.6 ± 0.8 Sv	0.36 ± 0.08 PW	0.12 ± 0.03 × 10^9 kg/s	0.14 ± 0.04 Sv	27.99°C

[a]Heat and freshwater transports are referenced to the temperature of 3.72°C and salinity of 34.62, respectively.

flow estimated in this study has a similar magnitude associated with the ITF as found by *Wyrtki* [1987]. As pointed out by *Wajsowicz* [1993] (in their section 4d), the depth-integrated steric height should decrease from north to south in the ITF region if friction is considered in *Godfrey*'s [1989] island rule. As shown by *Qu et al.* [2005] and *Wang et al.* [2006], the island rule can also be applied to the SCS throughflow. The existence of sea surface slope obtained from above calculation indicates that the friction is of importance in the "island rule" mechanism for the formation of the SCS branch of Pacific-to-Indian-Ocean throughflow.

6. Conclusions and Discussion

[24] 1. The observations show a mean volume transport of 3.6 Sv through the Karimata Strait (with the Gaspar Strait included) from the SCS to the ISs in the month from 13 January to 12 February 2008. This confirms the existence of the SCS branch of the Pacific-to-Indian-Ocean throughflow, or the SCS throughflow in boreal winter. This branch is of fundamental importance for the SCS oceanography in terms of the water mass formation, the air-sea heat and freshwater fluxes, and the flushing rate of the sea [*Fang et al.*, 2005]. With regard to the ITF, the Karimata Strait should be considered as an important inflow passage in addition to the Makassar Strait and the straits east of the Sulawesi Island.

[25] 2. Observations of currents in boreal summer are available at A_2 station. Although it is not adequate to estimate transport in boreal summer from the observations at this single point, we can still make a rough estimation using the monthly mean velocity shown in Table 2. If we assume that the volume transport is proportional to the vertically averaged along-channel velocity at A_2, then the maximum monthly mean volume transport in boreal summer should be around 1.7 Sv (northward). Therefore, the Karimata Strait throughflow, different from the Makassar Strait throughflow, provides positive volume (3.6 Sv, Table 3) to the ITF in boreal winter, but negative one in boreal summer. This indicates that the Karimata Strait transport can contribute a seasonal variability of more than 5 Sv in the total ITF transport.

[26] 3. The magnitude of annual mean volume transport through Karimata Strait is also one of our major concerns, because the mean transport is the net contribution of the SCS to the Indian Ocean. However, the current data at A_1 is too short to allow a reliable estimation. On the basis of the 10 month observed data at A_2, the annual mean of the vertically averaged along-channel velocity for the year from December 2007 to November 2008 is 8.1 cm/s (Table 2), while the volume transport through section A and the vertically averaged along-channel velocity at station A_2 for the month from 13 January to 12 February 2008 are 3.6 Sv and 35.0 cm/s, respectively. We can thus roughly estimate that the annual mean Karimata Strait transport is around 0.8 Sv for that year, provided that the volume transport is proportional to the vertically averaged velocity at A_2. Since this assumption may not be valid for the boreal summer months, this estimated value is subject to further verification, for example, by data assimilation. The Karimata Strait throughflow plays a double role in the total ITF volume transport, which is especially evident in boreal winter. The negative effect of the double role is that it can reduce the Makassar Strait transport as proposed by *Qu et al.* [2005] and *Tozuka et al.* [2007, 2009]; the positive effect is that the Karimata Strait throughflow itself can contribute volume transport to the ITF as proposed by *Fang et al.* [2005].

[27] 4. In comparison to the volume transport, the Karimata Strait throughflow plays an amplified double role in the ITF heat transport. The additional negative effect is that it can carry less saline (and thus less dense) water from the SCS, passing the Java Sea, to the southern mouth of the Makassar Strait to block the surface current from the Makassar Strait, and thus reduce the transport-weighted temperature of the Makassar Strait throughflow [*Gordon et al.*, 2003]. The additional positive effect is that the water carried by the Karimata Strait throughflow is much warmer than the Makassar Strait water owing to the shallowness of the Karimata Strait. Our estimation (Table 3) shows a mean heat transport of 0.36 PW through the Karimata Strait into ISs in a boreal winter month, with a transport-weighted temperature of 27.99°C. The combination of this inflow with the Makassar Strait throughflow can raise the transport-weighted temperature of the Makassar Strait throughflow from 16.6°C [*Gordon et al.*, 2008, Table 2] (their January–March values used) to 19.1°C of combined Makassar and Karimata straits throughflow. The latter is closer to the estimated transport-weighted temperature along IX1 line between Java and northwest Australia [*Wijffels et al.*, 2008].

[28] 5. So far, no accurate estimate of the freshwater transport associated with the ITF is available, though *Wijffels* [2001] gives a rough estimate of 0.2 Sv. The present study reveals a freshwater transport of 0.14 Sv in a boreal winter month. This suggests that the Karimata Strait transport is important in conveying freshwater toward the Indian Ocean in boreal winter. It should be mentioned here that this southward freshwater transport only occurs in boreal winter, and the annual mean is smaller. *Fang et al.* [2009] give an annual mean of 0.05 Sv on the basis of numerical model outputs. Furthermore, since the freshwater transport through the Luzon Strait is very small [*Fang et al.*, 2009], the source of the freshwater transported toward the ISs and finally to the Indian Ocean is from the SCS itself, namely the freshwater flux gain over the SCS and the land discharge surrounding the SCS.

[29] 6. The analysis of the boreal winter observations shows a downward sea surface slope from north to south. The sea surface gradient associated with the Karimata Strait throughflow has a magnitude close to that associated with the ITF found by *Wyrtki* [1987]. This result indicates the importance of friction in the "island rule" mechanism for the formation of the SCS branch of Pacific-to-Indian-Ocean throughflow.

Appendix A: Logarithmic-Profile-Cubic-Spline Interpolation/Extrapolation

[30] Let y represent the coordinate along the cross-channel section, with sidewalls designated as y = 0 and L. The velocities at $y = y_1, y_2, \ldots, y_N$ ($y_1 > 0$, and $y_N < L$) are known (N is equal to 2 in the present study):

$$u = u_1,\ u_2,\ \cdots,\ u_N \quad \text{at} \quad y = y_1, y_2,\ \cdots,\ y_N. \qquad \text{(A1)}$$

[31] We assume that the velocity in the intervals of $y \in [0, y_1]$ and $y \in [y_N, L]$ can be approximated by horizontal Prandtl's logarithmic profiles as in, for example, the work of *Charnock* [1959] for vertical profiles:

$$u = u_1 \frac{\ln[(y + l_0)/l_0]}{\ln[(y_1 + l_0)/l_0]}, \quad \text{for} \quad y \in [0, y_1], \tag{A2}$$

$$u = u_N \frac{\ln[(L - y + l_0)/l_0]}{\ln[(L - y_N + l_0)/l_0]}, \quad \text{for} \quad y \in [y_N, L], \tag{A3}$$

where l_0 is the roughness parameter. Equations (A2) and (A3) automatically satisfy $u = 0$, u_1, u_N, and 0 at $y = 0$, y_1, y_N, and L, respectively. Then the derivatives of u at points y_1 and y_N are

$$\frac{du}{dy} = \frac{u_1}{(y_1 + l_0)\ln[(y_1 + l_0)/l_0]}, \quad \text{at} \quad y = y_1, \tag{A4}$$

$$\frac{du}{dy} = \frac{-u_N}{(L - y_N + l_0)\ln[(L - y_N + l_0)/l_0]}, \quad \text{at} \quad y = y_N. \tag{A5}$$

Equation (A1), together with boundary conditions (A4) and (A5), can be used to interpolate velocity values using cubic-spline form in the segment of $y \in [y_1, y_N]$. This approach retains the continuity of first-order derivative of the function u at points y_1 and y_N, and thus over the entire section.

[32] From the observed vertical velocity profiles in the Red Wharf Bay, *Charnock* [1959] obtained the value of roughness parameter, which is ~0.3 cm. The horizontal scale of shelf sea is roughly in an order of 10^4 of the vertical scale. So the value of l_0 is estimated to be ~30 m. A sensitivity experiment was performed by taking l_0 = 10, 30, and 100 m, and revealed that the volume transport was insensitive to the choice of the roughness parameter: volume transport = 3.65, 3.63, and 3.61 Sv for l_0 = 10, 30, and 100 m, respectively. In the present study, the volume transport of 3.6 Sv is adopted.

[33] **Acknowledgments.** The authors sincerely thank the captains and crew of the research vessels *Baruna Jaya IV*, *I*, and *VIII* for their skillful operation during the voyages and their cooperation in fieldwork, and we thank all participants in the cruises. We also sincerely thank Quanan Zheng and Indroyono Soesilo for their efforts in establishing the SITE program. Comments by three anonymous reviewers greatly helped to improve the manuscript. The Chinese researchers of the SITE program are supported by the International Cooperative Program of the Ministry of Science and Technology under grant 2006DFB21630, the National Science Foundation of China under grant 40520140074, and the National Basic Research Program under contracts 2006CB40300 and 2011CB403500. The Indonesian researchers are supported by the Agency for Marine and Fisheries Research. The SITE program in the United States is funded by ONR-DURIP grant N0014-06-1-0738 and National Science Foundation grant OCE-07-51927.

References

Charnock, H. (1959), Tidal friction from currents near the seabed, *Geophys. J. R. Astron. Soc.*, *2*, 215–221.

Csanady, G. T. (1982), *Circulation in the Coastal Ocean*, 279 pp., D. Reidel, Dordrecht, Netherlands.

Fang, G., Z. Wei, B.-H. Choi, K. Wang, Y. Fang, and L. Wei (2002), Interbasin volume, heat and salt transport through the boundaries of the East and South China Seas from a variable-grid global ocean circulation model (in Chinese), *Sci. China, Ser. D*, *32*(12), 969–977.

Fang, G., D. Susanto, I. Soesilo, Q. Zheng, F. Qiao, and Z. Wei (2005), A note on the South China Sea shallow interocean circulation, *Adv. Atmos. Sci.*, *22*(6), 946–954, doi:10.1007/BF02918693.

Fang, G., Y. Wang, Z. Wei, Y. Fang, F. Qiao, and X. Hu (2009), Interocean circulation and heat and freshwater budgets of the South China Sea based on a numerical model, *Dyn. Atmos. Oceans*, *47*, 55–72, doi:10.1016/j.dynatmoce.2008.09.003.

Ffield, A., K. Vrancs, A. Gordon, and D. Susanto (2000), Temperature variability within Makassar Strait, *Geophys. Res. Lett.*, *27*(2), 237–240, doi:10.1029/1999GL002377.

Godfrey, J. S. (1989), A Sverdrup model of the depth-integrated flow for the world ocean allowing for island circulation, *Geophys. Astrophys. Fluid Dyn.*, *45*, 89–112, doi:10.1080/03091928908208894.

Gordon, A. L., R. D. Susanto, and K. Vranes (2003), Cool Indonesian Throughflow as a consequence of restricted surface layer flow, *Nature*, *425*, 824–828, doi:10.1038/nature02038.

Gordon, A. L., R. D. Susanto, A. Ffield, B. A. Huber, W. Pranowo, and S. Wirasantosa (2008), Makassar Strait throughflow, 2004 to 2006, *Geophys. Res. Lett.*, *35*, L24605, doi:10.1029/2008GL036372.

Indonesian Hydro-Oceanographic Service (2006), Indonesia Malaka Strait, Natuna Sea to Jawa Sea, *Chart 360*, Hydrographic-Oceanographic Service, Jakarta, Indonesia.

Lebedev, K. V., and M. I. Yaremchuk (2000), A diagnostic study of the Indonesian Throughflow, *J. Geophys. Res.*, *105*(C5), 11,243–11,258, doi:10.1029/2000JC900015.

Levitus, S., and T. Boyer (1994), *World Ocean Atlas*, 117 pp., Natl. Oceanic and Atmos. Admin., Washington, D. C.

Metzger, E. J., and H. E. Hurlburt (1996), Coupled dynamics of the South China Sea, the Sulu Sea, and the Pacific Ocean, *J. Geophys. Res.*, *101*(C5), 12,331–12,352, doi:10.1029/95JC03861.

Milliff, R. F., and J. Morzel (2001), The global distribution of the average wind stress curl from NSCAT, *J. Atmos. Sci.*, *58*, 109–131, doi:10.1175/1520-0469(2001)058<0109:TGDOTT>2.0.CO;2.

Milliff, R. F., W. G. Large, J. Morzel, G. Danabasoglu, and T. M. Chin (1999), Ocean general circulation model sensitivity to forcing from scatterometer winds, *J. Geophys. Res.*, *104*(C5), 11,337–11,358, doi:10.1029/1998JC900045.

Qu, T., Y. Du, G. Meyers, A. Ishida, and D. Wang (2005), Connecting the tropical Pacific with Indian Ocean through South China Sea, *Geophys. Res. Lett.*, *32*, L24609, doi:10.1029/2005GL024698.

Qu, T., Y. T. Song, and T. Yamagata (2009), An introduction to the South China Sea throughflow: Its dynamic, variability, and application for climate, *Dyn. Atmos. Oceans*, *47*, 3–14, doi:10.1016/j.dynatmoce.2008.05.001.

Schiller, A., I. S. Godfrey, P. C. McIntosh, G. Meyers, and S. E. Wijffels (1998), Seasonal near-surface dynamics and thermodynamics of the Indian Ocean and Indonesian Throughflow in a global ocean general circulation model, *J. Phys. Oceanogr.*, *28*, 2288–2312, doi:10.1175/1520-0485(1998)028<2288:SNSDAT>2.0.CO;2.

Song, Y. T. (2006), Estimation of interbasin transport using ocean bottom pressure: Theory and model for Asian marginal seas, *J. Geophys. Res.*, *111*, C11S19, doi:10.1029/2005JC003189.

Sprintall, J., S. E. Wijffels, R. Molcard, and I. Jaya (2009), Direct estimates of the Indonesian Throughflow entering the Indian Ocean: 2004–2006, *J. Geophys. Res.*, *114*, C07001, doi:10.1029/2008JC005257.

Susanto, R. D., G. Fang, I. Soesilo, Q. Zheng, F. Qiao, Z. Wei, and B. Sulistyo (2010), New surveys of a branch of the Indonesian Throughflow, *Eos Trans. AGU*, *91*(30), 261, doi:10.1029/2010EO300002.

Tozuka, T., T. Qu, and T. Yamagata (2007), Dramatic impact of the South China Sea on the Indonesian Throughflow, *Geophys. Res. Lett.*, *34*, L12612, doi:10.1029/2007GL030420.

Tozuka, T., T. Qu, Y. Masumoto, and T. Yamagata (2009), Impacts of the South China Sea throughflow on seasonal and interannual variations of the Indonesian Throughflow, *Dyn. Atmos. Oceans*, *47*, 73–85, doi:10.1016/j.dynatmoce.2008.09.001.

Wajsowicz, R. C. (1993), The circulation of the depth-integrated flow around an island with application to the Indonesian Throughflow, *J. Phys. Oceanogr.*, *23*, 1470–1484, doi:10.1175/1520-0485(1993)023<1470:TCOTDI>2.0.CO;2.

Wang, D., Q. Liu, R. X. Huang, Y. Du, and T. Qu (2006), Interannual variability of the South China Sea throughflow inferred from wind data and an ocean data assimilation product, *Geophys. Res. Lett.*, *33*, L14605, doi:10.1029/2006GL026316.

Wijffels, S. E. (2001), Ocean transport of fresh water, in *Ocean Circulation and Climate*, edited by G. Siedler et al., pp. 475–488, doi:10.1016/S0074-6142(01)80135-2, Academic, San Diego, Calif.

Wijffels, S. E., G. Meyers, and J. S. Godfrey (2008), A 20-yr average of the Indonesian Throughflow: Regional currents and the interbasin exchange, *J. Phys. Oceanogr.*, *38*, 1965–1978, doi:10.1175/2008JPO3987.1.

Wyrtki, K. (1961), Physical oceanography of Southeast Asian waters, in *NAGA Report: Scientific Results of Marine Investigations of the South China Sea and Gulf of Thailand*, vol. 2, Scripps Inst. of Oceanogr., La Jolla, Calif.

Wyrtki, K. (1987), Indonesian through flow and the associated pressure gradient, *J. Geophys. Res.*, *92*(C12), 12,941–12,946, doi:10.1029/JC092iC12p12941.

Yaremchuk, M., J. McCreary Jr., Z. Yu, and R. Furue (2009), The South China Sea throughflow retrieved from climatological data, *J. Phys. Oceanogr.*, *39*, 753–767, doi:10.1175/2008JPO3955.1.

Yu, Z., S. Shen, J. P. McCreary, M. Yaremchuk, and R. Furue (2007), South China Sea throughflow as evidenced by satellite images and numerical experiments, *Geophys. Res. Lett.*, *34*, L01601, doi:10.1029/2006GL028103.

B. Fan, G. Fang, S. Li, F. Qiao, and Z. Wei, Key Laboratory of Marine Science and Numerical Modeling, The First Institute of Oceanography, State Oceanic Administration, 6 Xian-Xia-Ling Rd., Qingdao, Shandong 266061, China. (fanggh@fio.org.cn)

B. Sulistiyo, A. Supangat, and S. Wirasantosa, Agency for Marine and Fisheries Research, Ministry of Marine Affairs and Fisheries, Jakarta, 12770, Indonesia.

R. D. Susanto, Lamont-Doherty Earth Observatory, Earth Institute at Columbia University, Palisades, NY 10964, USA.